



# Study on Longitudinal Collision Risk of Closely Spaced Parallel Runways Paired Approach

Fei LU<sup>1</sup>, Jian ZHANG<sup>2</sup>, Erli ZHAO<sup>3</sup>, Jingjie TENG<sup>4</sup>

Original Scientific Paper  
Submitted: 16 May 2024  
Accepted: 28 Aug 2024

<sup>1</sup> Corresponding author, lufei315@126.com, Civil Aviation University of China, College of Air Traffic Management

<sup>2</sup> zhangjian@cauc.edu.cn, Civil Aviation University of China, College of Air Traffic Management

<sup>3</sup> zhaoel1002@163.com, Civil Aviation University of China, College of Air Traffic Management

<sup>4</sup> tengjj1103@163.com, Civil Aviation University of China, College of Air Traffic Management



This work is licenced under a Creative Commons Attribution 4.0 International Licence.

Publisher:  
Faculty of Transport and Traffic Sciences,  
University of Zagreb

## ABSTRACT

This study asserts that paired aircraft can withstand specific wake turbulence levels and explores the longitudinal collision risk in closely spaced parallel runway approaches. The goal is to enhance the safety margin of the paired approach and allow for more flexible implementation. Based on QAR data, a theoretical spacing model for paired aircraft and a probability distribution of acceleration error are established to facilitate the analysis of the actual spacing of paired aircraft. Wake turbulence attenuation is modelled using large eddy simulation, creating a vortex attenuation model. Drawing inspiration from the Hallock-Burnham vortex model, new models for induced velocity and vortex core motion are proposed. The study assumes that trailing aircraft can handle certain wake intensities, leading to a new model for calculating wake turbulence safety intervals, limiting the trailing aircraft's maximum roll angle to its critical limit. Using probability theory, a model for longitudinal collision risk is formulated, combining wake turbulence safety separation and the actual separation of paired aircraft. The study also examines various factors influencing longitudinal collision risk, emphasising the significant impact of crosswind conditions. It concludes that a stronger crosswind component reduces the wake turbulence safety separation, thereby increasing the risk of longitudinal collisions, particularly during the final stage of the approach. Notably, collision risk is directly proportional to the crosswind component and initial longitudinal separation, but inversely proportional to runway spacing.

## KEYWORDS

paired approach; collision risk; wake vortex filed; safety interval; acceleration errors; roll moment.

## 1. INTRODUCTION

Closely spaced parallel runways (CSPRs) are defined as parallel runways with intervals ranging from 213 meters to 760 meters. Currently, most CSPRs operate in a mode of isolated parallel operations, where one runway is designated exclusively for departures and the other for approaches. This mode somewhat enhances airport approach capacity but does not fully capitalise on the benefits of parallel runways. Consequently, the CSPRs program has been initiated. While this program significantly improves the airport's landing capacity, the separation between the leading and trailing aircraft during its implementation is notably smaller compared to traditional approaches. Therefore, to enhance approach efficiency without compromising safety, a thorough evaluation of the safety of the paired approach process is essential.

The concept of a paired approach for closely spaced parallel runways was first introduced by NASA in 1996 [1]. Subsequent research has extensively explored this concept. Hammer provided a detailed elaboration of the program and analysed its safety, emphasising collision avoidance and wake turbulence

from the leading aircraft. His studies indicated that a trailing aircraft can more effectively avoid the wake of the leading aircraft by approaching at an offset angle of  $3^\circ$  [2, 3]. Additionally, Landry et al. [4] introduced the concept of a safety zone for the paired approach procedure. Their research systematically examined the impact of factors such as aircraft dynamics, pilot operating proficiency and wake dissipation mechanisms on the safety zone range. In addition, Burnham et al. [5] developed a wake dissipation model utilising existing data on wake lateral transfer. This model evaluates the relationship between the longitudinal interval and crosswind in paired approaches and explores the effects of wake on closely spaced parallel runways under crosswind conditions. McKissick [6] employed the Monte Carlo method to simulate the trajectory of aircraft from the final approach fix to the threshold, revealing that most wake encounters occur near or above the runway. Lastly, Liu [7] focused on the practical significance and feasibility of the paired approach from an air traffic control perspective, examining parameters including air traffic control equipment error and wake effects on the paired approach. Guerreiro et al. [8, 9] initially explored the wake safety zone using the Monte Carlo method. Subsequent research included simulation experiments on the horizontal motion characteristics of the wake and an evaluation of the wake safety interval. Lu et al. [10–13] developed a model for the actual separation of paired approaching aircraft based on position error theory. They examined the distribution of positioning errors in conjunction with the paired approach process. By accounting for the effects of crosswinds and the wake turbulence of the leading aircraft, they assessed the lateral and longitudinal collision risks in paired approaches. Furthermore, they established a moment balance equation, assuming the aircraft could withstand a specific intensity of wake turbulence. By integrating the moment balance equation with the distribution of aircraft position errors, they created a safety assessment model to determine the safe separation distances for paired approaches. Additionally, Tian et al. [14] proposed methods for determining runway centreline spacing and staggered spacing at runway entrances, based on the characteristics of wake movement in the most disadvantageous conditions. Domino & Tuomey et al. [15] assessed the initial feasibility of flight crews executing the paired approach procedure through simulation, finding that both pilots and controllers could effectively perform their tasks within acceptable workload limits. The results suggest that a steady-state capacity of over 45 aircraft per hour might be achievable with this procedure, even down to Category I minima. Between 2018 and 2019, entities including United Airlines, Mosaic Air Traffic Control Company and Honeywell Company conducted test flights of paired approaches at San Francisco International Airport. They collected extensive data from communications, navigation and surveillance (CNS) equipment, controllers and crew, providing a safety foundation for the specific implementation of the paired approach mode [16, 17].

The concept of the CSPRs paired approach, previously only theoretical and not yet implemented, has led to assumptions about aircraft movement and position error distribution during the approach. This paper utilises quick access recorder (QAR) data to analyse aircraft movement in the final approach stage, establishing models for speed change and theoretical intervals of paired aircraft. Additionally, the study fits a probability distribution to the aircraft speed changes recorded in the QAR data, thereby computing the actual interval distribution between the leading and trailing aircraft. Previous research on the safety interval of the paired approach mandated that the trailing aircraft should not enter the wake of the leading aircraft, resulting in conservative safety interval calculations. However, in reality, aircraft can tolerate wakes of certain intensities. This paper introduces a wake safety interval model that considers the trailing aircraft's response mechanism after encountering the leading aircraft's wake, using the maximum roll angle of the trailing aircraft as a critical value to calculate the wake safety interval. This approach broadens the safety range for the paired approach compared to previous studies.

The structure of this paper is as follows: Section 2 presents an analysis of aircraft motion processes based on QAR data. Section 3 details the models and methods used. Section 4 introduces the analysis and results of wake turbulence separation and longitudinal collision risk in the paired approach. Finally, section 5 offers the conclusion.

## 2. MOVEMENT PROCESS ANALYSIS OF PAIRED AIRCRAFT BASED ON QAR DATA

The paired approach procedure begins when the lead aircraft reaches the final approach fix (FAF) and ends at the missed approach point (MAPt). Throughout this procedure, the trailing aircraft maintains a specified separation from the lead aircraft, flying to the MAPt at a glide slope of  $3^\circ$ .

Given that the CSPRs paired approach has not yet been implemented in practice, this paper focuses on intercepting QAR data from the final approach stage of traditional approaches. QAR data from 78 Boeing

737–800 aircraft landings at Tianjin Binhai International Airport were analysed, focusing on their speed variations from the FAF. The average speed of these 78 aircraft was calculated to examine the trend of speed changes, as depicted by the solid black line in *Figure 2*. The analysis revealed that the aircraft underwent a rapid deceleration approximately 30 seconds after the FAF, identified as the 0–time point. This deceleration becomes more gradual from this point until reaching the MAPt. In these two phases, the speed variation pattern of the aircraft is characterised by a linear decrease. Consequently, the paper categorises the aircraft’s motion between the FAF and MAPt into two distinct phases based on differing deceleration rates.

To determine the transition point  $t_k$  between these phases more precisely, a cluster analysis of acceleration was performed, with the results presented in *Figure 1*. Different colours in the figure indicate accelerations belonging to various categories. Based on these findings, the precise cut-off point between the two stages is identified as  $t_k = 32.5$ . However, due to the lack of sample data on the aircraft’s true airspeed after 140 seconds, the acceleration data in this later stage is not considered reliable for analysis.

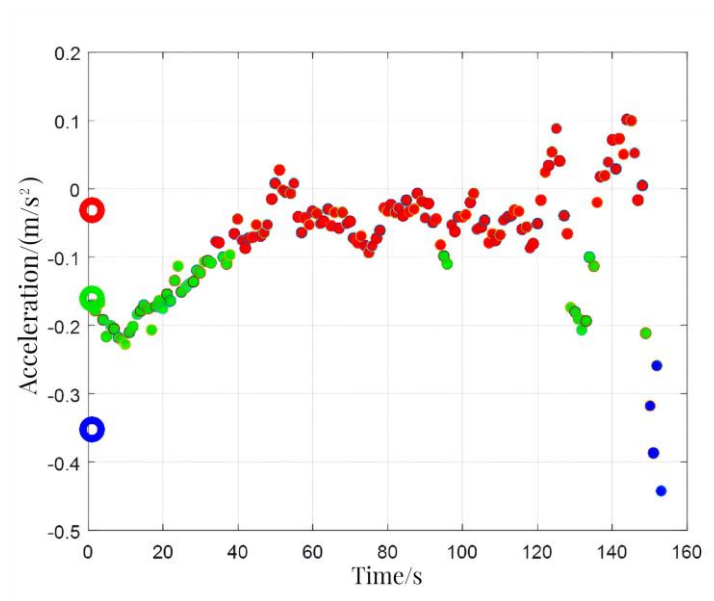


Figure 1 – Acceleration cluster analysis diagram

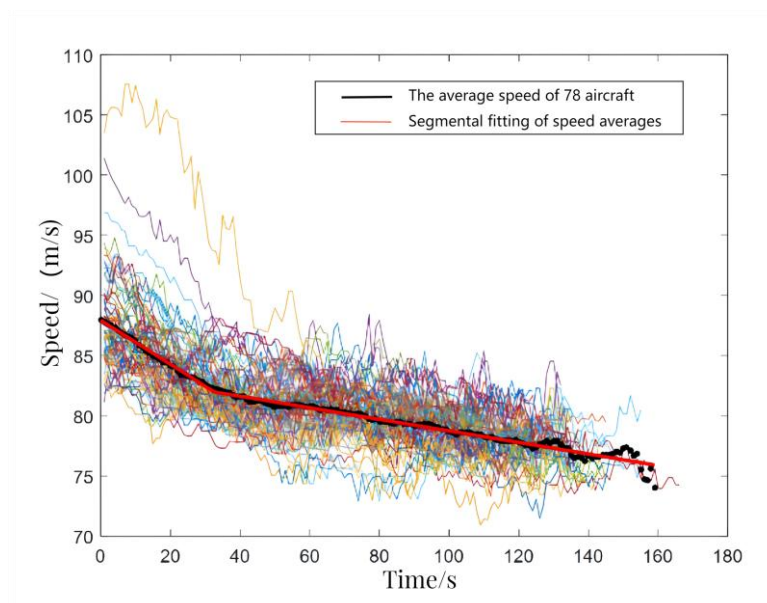


Figure 2 – Motion process fitting

For the identified cut-off point  $t_k$ , a polynomial segmentation fitting is applied to the average true airspeed, with the outcomes depicted as the red solid line in *Figure 2*. The speed variation of the aircraft during the approach process can thus be determined.

### 3. MODELS AND METHODS

#### 3.1 Longitudinal separation model of paired aircraft

##### *Kinematic model of paired aircraft*

Combined with the law of speed change in section 2, the acceleration change of the leading and trailing aircraft in the process of paired approach can be obtained:

$$\begin{cases} a_{1j}(t) = \begin{cases} a_{11}, t \in T_{11} \\ a_{12}, t \in T_{21} \end{cases} \\ a_{2j}(t) = \begin{cases} a_{21}, t \in T_{12} \\ a_{22}, t \in T_{22} \end{cases} \end{cases} \quad (1)$$

where  $a_{ij}(t)$  is the acceleration of the leading and trailing aircraft before and after the time  $t_k$  and  $T_{ij}$  is the time interval of the deceleration stage before and after the time  $t_k$ .

By integrating the acceleration, the speed variation for both the leading and trailing aircraft can be determined as:

$$\begin{cases} V_1(t) = V_{1i} + \int_0^t a_1(t) dt \\ V_2(t) = V_{2i} + \int_0^t a_2(t) dt \end{cases} \quad (2)$$

where  $V_1(t)$  is the true airspeed of the leading aircraft at time  $t$ ,  $V_2(t)$  is the true airspeed of the trailing aircraft at time  $t$ ,  $V_{1i}$  is the initial approach speed of the leading aircraft, and  $V_{2i} = \sqrt{V_{1i}^2 - 2a_{21}s_0}$  is the initial approach speed of the trailing aircraft.  $T_{11} = [0, t_k]$  is the time interval for the first deceleration stage of the leading aircraft.  $T_{12} = [t_k, t_f]$  is the time interval for the second deceleration stage of the leading aircraft.  $T_{21} = [0, t_k - \frac{V_{2i} - V_{1i}}{a_{21}}]$  is the time interval for the first deceleration stage of the trailing aircraft.

$T_{22} = [t_k - \frac{V_{2i} - V_{1i}}{a_{21}}, t_f]$  is the time interval for the second deceleration stage of the trailing aircraft.

##### *Theoretical separation calculation of aircraft*

In the process of paired approach, both aircraft maintain a specified initial longitudinal safety interval  $s_0$ , sequentially decelerating and descending at a designated glide angle  $\vartheta$ . Throughout this phase, the trailing aircraft executes its approach at an offset angle of  $3^\circ$  until it decelerates to its final approach speed. The procedure culminates when the leading aircraft reaches the threshold. To facilitate the analysis of the separation between the leading and trailing aircraft, this study establishes a coordinate system centred around the leading aircraft. During the paired approach process, the position coordinates of the leading aircraft are defined as  $(0, 0, 0)$ , establishing it as the reference point in the coordinate system. Meanwhile, the position coordinates of the trailing aircraft are denoted by  $[X(t), Y(t), Z(t)]$ , where  $X(t)$  represents lateral separation,  $Y(t)$  indicates longitudinal separation, and  $Z(t)$  signifies vertical separation from the leading aircraft. Utilising the geometric relationship between the positions of the leading and trailing aircraft, along with their respective models of speed change, a separation model between the two aircraft can be formulated as follows:

$$\begin{cases} X(t) = h + (l + s_0) \tan \beta - \int_0^t V_2(t) \sin \beta dt \\ Y(t) = s_0 + \int_0^t V_1(t) - V_2(t) \cos \beta dt \\ Z(t) = s_0 \sin \delta - \int_0^t [V_2(t) - V_1(t)] \sin \delta dt \end{cases} \quad (3)$$

where  $h$  is runway spacing and  $l = \int_0^t V_1(t) \cos \delta dt$  is the distance from the final approach fix point to the threshold.

*Acceleration error distribution of the aircraft*

Longitudinal position errors in aircraft are primarily caused by acceleration errors. During the final approach phase, the pilot continuously adjusts speed to comply with landing requirements. In this study, QAR-recorded speeds of 78 flights were averaged, the average acceleration was calculated as the preset value, and the acceleration deviation at each moment was considered the acceleration error. Statistical analysis shows that the error distribution of acceleration, as depicted in *Figure 3*, reveals multiple peaks, indicating that fitting it to a normal distribution is insufficiently precise. Therefore, a mixed normal distribution and a mixed Laplace distribution were used for fitting, and each fitting effect was compared using a cumulative distribution probability plot, as shown in *Figure 4*. The results show that the mixed Laplace distribution was most consistent with the distribution of acceleration deviation values and provided the best fitting effect. Thus, the mixed Laplace distribution was selected. The fitting results using the mixed Laplace distribution are presented as follows:

$$\begin{aligned} f(\varepsilon_y) = & 0.156 * \frac{1}{2 * 0.1048} \exp\left(-\frac{|\varepsilon_y + 0.5|}{0.1048}\right) + 0.2995 * \frac{1}{2 * 0.1279} \exp\left(-\frac{|\varepsilon_y|}{0.1279}\right) \\ & + 0.1876 * \frac{1}{2 * 0.1952} \exp\left(-\frac{|\varepsilon_y - 0.5|}{0.1952}\right) + 0.1882 * \frac{1}{2 * 0.4007} \exp\left(-\frac{|\varepsilon_y + 1|}{0.4007}\right) \\ & + 0.1687 * \frac{1}{2 * 0.6152} \exp\left(-\frac{|\varepsilon_y - 1.1|}{0.6152}\right) \end{aligned} \quad (4)$$

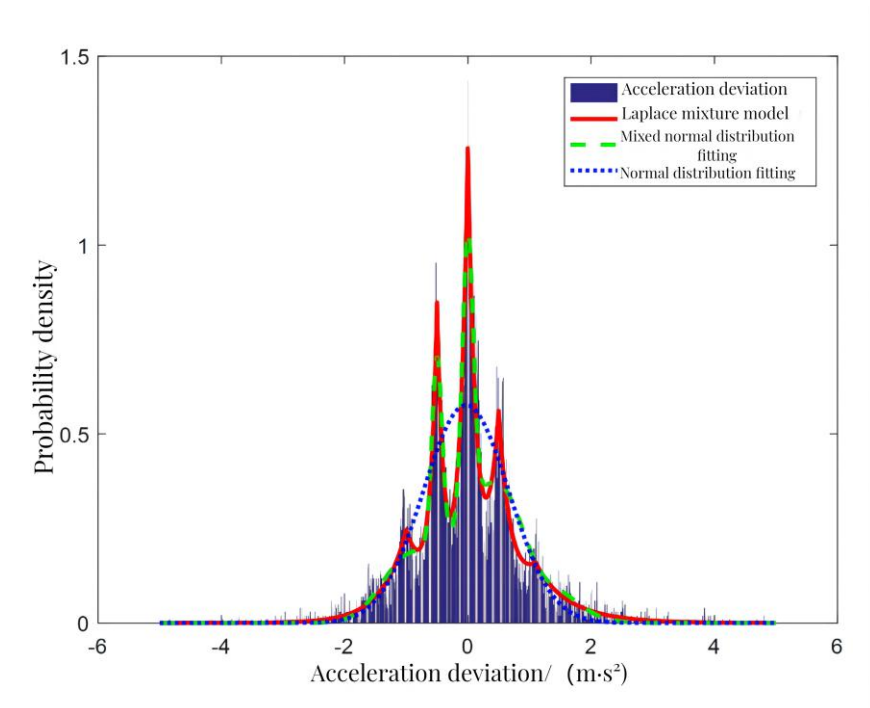


Figure 3 – Acceleration error distribution

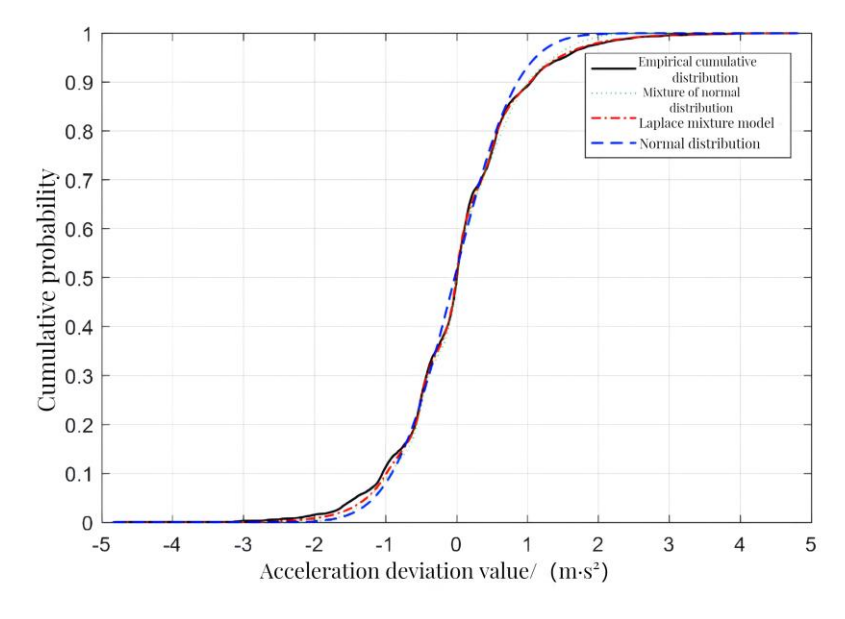


Figure 4 – Cumulative probability distribution of different methods

### 3.2 Wake safety interval model

#### Modelling the state of motion of the wake

The initial intensity of a single wake vortex generated by the leading aircraft during the paired approach is quantified by the following Equation 5:

$$\Gamma_0(t) = \frac{m_1 g}{\rho V_1(t) B_1 s} \tag{5}$$

here,  $\Gamma_0(t)$  represents the initial circulation of the wake produced by the leading aircraft at instant  $t$ . The variable  $m_1$  denotes the weight of the leading aircraft,  $g$  is the gravitational acceleration,  $\rho$  symbolizes atmospheric density,  $B_1$  refers to the wingspan of the leading aircraft, and  $s$  is the characteristic parameter of the wing. For swept-wing aircraft,  $s$  is typically considered to be  $\pi/4$ .

To analyse the wake attenuation law, a numerical simulation of the wake field during the approach phase of paired aircraft is conducted using the large eddy simulation method on the ANSYS software platform. This simulation assesses the variation in wake intensity as a function of distance, leading to a fitting of the trend. The resulting equation is expressed as follows:

$$\Gamma_t(d) = \Gamma_{c0} \bullet \exp\left(-\frac{0.15d}{v_\infty}\right) \tag{6}$$

here,  $\Gamma_t(d)$  signifies the vortex value of the wake at a distance  $D$  from the leading aircraft at time  $t$ ,  $\Gamma_{c0}$  represents the maximum vortex value at the reference cross-section, and  $v_\infty$  denotes the incoming flow velocity.

The wingtip vortex tends to move backwards and downwards, with the downward motion primarily caused by mutual induction between the two vortices. Side winds significantly affect the drift of the vortex core, and the velocity model of the vortex core is developed by incorporating these factors:

$$\begin{cases} V_x = V_{ex} \\ V_y = V_\infty + V_{ey} \\ V_z = -\frac{\Gamma_0(t)}{2\pi b_1} + V_{ez} \end{cases} \tag{7}$$



here,  $V_{ex}$ ,  $V_{ey}$  and  $V_{ez}$  respectively represent the lateral, longitudinal and vertical components of the crosswind's speed. The symbol  $V_i$  denotes the speed of the vortex core movement, where  $i=x$  corresponds to the lateral component,  $i=y$  to the longitudinal component and  $i=z$  to the vertical component.

During the paired approach, the calculation model for the coordinates of the right vortex core  $(S_{Y(t)x}, S_{Y(t)y}, S_{Y(t)z})$  at a longitudinal interval  $Y(t)$  from the leading aircraft is formulated as follows:

$$\begin{cases} S_{Y(t)x} = \frac{B_1}{2} + \int_0^{Y(t)} \frac{V_x}{V_1(t)+V_{ey}} dt \\ S_{Y(t)y} = Y(t) \\ S_{Y(t)z} = \int_0^{Y(t)} \frac{V_z}{V_1(t)+V_{ey}} dt \end{cases} \quad (8)$$

The Hallock-Burnham vortex model [19] defines the induced velocity imparted by a point vortex in a real fluid to a specific point in space. This is mathematically expressed as:

$$V = \frac{r\Gamma}{2\pi(r^2 + r_c^2)} \quad (9)$$

here,  $r_c$  signifies the radius of the vortex core, and  $r$  represents the distance from a point in space to the centre of the vortex core.

In the paired approach procedure, only the side of the trailing aircraft proximate to the leading aircraft intersects the frontal tail vortex field. The wingtip vortices from both aircraft have opposite rotational directions, resulting in the generation of two induced velocities with opposing directions at a specific point on the trailing aircraft's rear wing. Additionally, the component of induced velocity perpendicular to the wing significantly influences the aircraft's roll. Under the assumption that the strengths of the two wingtip vortices from the leading aircraft are identical, their combination with the vortex core position model and the Hallock-Burnham vortex model facilitates the calculation of the induced velocity at a specific point on the wing of the trailing aircraft. This point's position relative to the leading aircraft is given by the coordinates  $[X(t), Y(t), Z(t)]$ , and the induced velocity is determined as follows:

$$V(y) = \frac{\Gamma_{Y(t)}[X(t) - S_{Y(t)x} + y]}{2\pi\{[X(t) - S_{Y(t)x} + y]^2 + [S_{Y(t)z} - Z(t)]^2 + r_c^2\}} - \frac{\Gamma_{Y(t)}[X(t) - S_{Y(t)x} + B_1 + y]}{2\pi\{[X(t) - S_{Y(t)x} + B_1 + y]^2 + [S_{Y(t)z} - Z(t)]^2 + r_c^2\}} \quad (10)$$

here,  $y$  represents the spanwise coordinate of a point on the wing of the trailing aircraft.

#### Establishment of wake safety interval model

When the trailing aircraft encounters the wake vortex of the leading aircraft due to positional error, an induced roll moment  $R$  is generated, causing the aircraft to roll. Simultaneously, a damping moment  $T$  is generated by the aircraft to resist the roll. Upon detecting the roll, the pilot manoeuvres the control stick to deflect the ailerons, thereby producing a manoeuvring moment  $M$ . The pilot's reaction time is denoted as  $t_e$  [20].

The angle of approach of the trailing aircraft changes when it is within the aft vortex field of the leading aircraft, resulting in a change in wing lift. As the induced velocity decreases with distance from the vortex core, the change in lift on the left and right wings of the trailing aircraft differs, generating two moments of different magnitudes relative to the aircraft's centre, thereby causing a roll. By calculating the moments on the left and right wings of the trailing aircraft and subtracting the results, the induced roll moment  $R(t)$  of the trailing aircraft at a given time  $t$  can be determined.

$$R(t) = \frac{1}{2} \rho V_2(t) C_L^\alpha \int_{-B_2/2}^{B_2/2} V(y) b(y) y dy \tag{11}$$

Here,  $B_2$  represents the rear wingspan, and  $b(y)$  indicates the chord length of the rear wing profile. Considering the positional relationship between the leading and trailing aircraft during the paired approach, within the coordinate system established in this paper, the variable  $b(y)$  can be articulated using Equation 12:

$$b(y) = \frac{2S_w [B_2 + B_2 \lambda - 2|y|(1 - \lambda)]}{B_2^2 (1 + \lambda)} \tag{12}$$

here,  $\lambda$  is the taper ratio, and  $S_w$  denotes the wing area.

The damping moment, generated along with the induced roll moment, acts as a hindrance to the roll of the aeroplane and can be calculated using the following Equation 13 [21]:

$$T(t) = \frac{1}{4} \rho V_2(t) S_w B_2^2 w C_{rp} \tag{13}$$

here,  $w$  represents the roll angular velocity, and  $C_{rp}$  is the coefficient representing the damping moment.

The manoeuvring moment is primarily generated by aileron deflection and can be expressed as:

$$M(t) = C_L^\alpha \eta_x \partial_x \rho V_2(t)^2 S_x l_0 \tag{14}$$

where  $l_0$  is the lateral distance of the aileron centre from the longitudinal axis (m),  $C_L^\alpha$  is the slope of the lift line,  $\eta_x$  is the aileron efficiency,  $\partial_x$  is the aileron deflection angle ( $^\circ$ ), and  $S_x$  is the total surface area of the aileron ( $m^2$ ).

The position of the trailing aircraft is defined as the wake safety interval when the roll angle of the aircraft equals the critical roll angle  $\gamma_m$ . The initial roll angular acceleration of the trailing aircraft upon first encountering the wake is considered to be 0. The initial roll angular acceleration of the trailing aircraft upon first encountering the wake stream is considered to be  $a_0$ , with the roll angular velocity  $w$  at 0 and the aircraft's roll angle  $\gamma$  also at 0. The roll angular acceleration is defined as the combined roll moment divided by the rotational moment of inertia [22].

After the pilot's reaction time, the aircraft is manoeuvred by the pilot to produce a manoeuvring moment, and the roll angular acceleration of the aircraft is given by:

$$a_w = \frac{R(t) - T(t) - M(t)}{I} \tag{15}$$

By resolving the differential equation pertaining to the aircraft's roll dynamics, the roll angle of the aircraft can be calculated as follows:

$$\gamma(t) = \frac{R(t)I}{A^2} \exp\left(-\frac{A}{I}t\right) - \frac{M(t)I}{A^2} \exp\left[\frac{A}{I}(t - t_e)\right] + \frac{R(t) - M(t)}{A} t + \frac{M(t)}{A} t_e - \frac{R(t) - M(t)}{A^2} \tag{16}$$

$$A = \frac{1}{4} \rho V_2(t) S_w B_2^2 C_{rp} \tag{17}$$

In the process of calculating the wake safety interval in a particular direction, it is important to note that while the intervals between the two aircraft in the other two directions remain constant, the interval in the direction under consideration is variable. This allows for the deduction of the induced roll moment  $R(t)$  at



various instances  $t$ . Subsequently, the wake safety interval  $Q(t)$  at each point in time can be determined by integrating Equations 10 and 11. The resulting expression for the roll angle of the aircraft is formulated as follows:

$$\gamma(t') = \begin{cases} \gamma(t')_{\max} = \gamma_m \\ \frac{R(t)I}{A^2} \exp(-\frac{A}{I}t') + \frac{R(t)}{A}t' - \frac{R(t)I}{A^2}, t' \leq t_e \\ \frac{R(t)I}{A^2} \exp(-\frac{A}{I}t') - \frac{M(t)I}{A^2} \exp\left[\frac{A}{I}(t' - t_e)\right] + \frac{R(t) - M(t)}{A}t' + \frac{M(t)}{A}t_e - \frac{R(t) - M(t)}{A^2}, t' > t_e \end{cases} \quad (18)$$

here,  $y$  represents the spanwise coordinate of a point on the wing of the trailing aircraft.

### 3.3 Longitudinal collision risk assessment model of CSPRs paired approach

In the paired approach procedure, the trailing aircraft must stay ahead of the leading aircraft's wake to avoid it effectively. A collision is considered to have occurred if either the fuselages of the two aircraft come into contact or if the trailing aircraft loses control due to the wake of the leading aircraft. To successfully implement the paired approach procedure, the longitudinal interval between the two aircraft must satisfy the following criteria:

- (1) Avoid fuselage contact: The trailing aircraft should maintain a sufficient distance from the leading aircraft to prevent any possibility of collision.
- (2) Prevent the loss of control in the wake: The trailing aircraft must keep an optimal distance from the leading aircraft. This distance should be close enough to allow the trailing aircraft to recover a stable attitude if affected by the wake, yet far enough to ensure safety.

During the study of longitudinal collision risk in paired aircraft approach, the following assumptions are made:

- (1) Independent acceleration errors: Once the two aircraft have completed pairing, their respective acceleration errors are assumed to be mutually independent [15, 16];
- (2) Uniform operating environment: The operating environment is considered to have a consistent impact on both paired aircraft;
- (3) Consistent pilot skill levels: The study does not take into account variations in pilots' operational skills.

At any moment  $t$ , the theoretical longitudinal separation between the front and rear aircraft is  $Y(t)$ . However, the actual longitudinal separation  $Y_c(t)$  will deviate from  $Y(t)$  due to the aircraft's acceleration error  $\varepsilon_y$ . Assuming the position of the leading aircraft remains unchanged and the trailing aircraft operates with twice the acceleration error, the actual longitudinal separation of the trailing aircraft will be  $Y_c(t) = Y(t) + 2 \times \frac{1}{2} \varepsilon_y t^2$ . In actual operations, due to diligent monitoring by controllers and attentive observation by pilots, it is unlikely for an aircraft to deviate significantly from its predetermined speed for an extended period. The adjustment time to rectify any deviation is denoted as  $t_r$ , and the actual interval of the trailing aircraft is represented as  $Y_c(t) = Y(t) + 2 \times \frac{1}{2} \varepsilon_y t_r^2$ . The probability density function of acceleration error, derived from QAR data, is labelled as  $f(\partial_y)$ , while the probability density function  $f[Y_c(t)]$  of  $Y_c(t)$  is indicated as  $f\left[\frac{Y_c(t) - Y(t)}{t_r^2}\right]$ . A collision is predicted to occur within the actual interval range  $[C_1, C_2]$ . Thus, the longitudinal collision probability of the paired approach at a specific instant  $t$  can be calculated.

$$P_y(t) = \int_{C_1}^{C_2} f[Y_c(t)] dY_c(t) \quad (19)$$

The analysis leads to the conclusion that the longitudinal collision interval  $[Y_1, Y_2]$  is defined as  $\{Q_{1y}, +\infty\}$ , based on the premise that a single collision equates to two separate accidents. Therefore, the longitudinal collision risk of the paired approach is expressed as  $P_{CSPAY}(t) = 2NP_y(t)$ .

In summary, the longitudinal collision risk assessment model for the paired approach is established as follows:

$$\left\{ \begin{array}{l} P_{CSPAY}(t) = 2NP_y(t) \\ N = 1 + \frac{t_f}{t_s} \\ P_y(t) = \int_{Y_1}^{Y_2} f[Y_c(t)] dY_c(t) \\ Y_2 = +\infty \\ Y_1 = Q_{1y}(t) \end{array} \right. \quad (20)$$

here,  $t_s$  is the time interval considered necessary after the dissipation of wake turbulence from the current paired aircraft before initiating the next paired approach.

## 4. ANALYSIS AND RESULTS

### 4.1 Analysis of wake safety interval

#### *Influence of crosswind on longitudinal wake safety interval*

In the process of calculating the longitudinal wake interval for aircraft using the proposed model, this study assumes that the vertical and lateral positions of the aircraft are at their theoretical locations, disregarding any position errors in these two directions. However, for the longitudinal interval  $Y(t)$ , which is the variable under consideration, it is essential to compute the solution for  $Q(t)$  – the wake safety interval at time  $t$ . Acceleration errors can cause the trailing aircraft to deviate longitudinally from its intended trajectory. When the trailing aircraft deviates from its position by more than  $Q(t)$ , the roll angle of the aircraft exceeds the critical roll angle due to the increasing induced torque. At this point, the aircraft is unable to regain stability and consequently loses control.

The motion of the vortex core of the leading aircraft is affected by the crosswind. The vertical component of the crosswind affects the vertical distance between the trailing aircraft and the vortex core, while the lateral component affects the lateral distance. For simplicity, a single vortex core is considered. When the lateral component of the crosswind is zero, the wake vortex core does not drift with the wind towards the trailing aircraft, thus maintaining a substantial lateral distance. Consequently, the induced roll moment on the trailing aircraft is minimal and does not significantly impact its operation. Similarly, when the vertical component of the crosswind is zero, the induced roll moment experienced by the trailing aircraft is negligible, posing no substantial effect on its operation. When the vortex core is in the plane of the wing, the effective component of the induced velocity on the wingtip is maximal. Therefore, this study refers to the vertical component  $V'_{ez}$  of the crosswind blowing towards this position as the most unfavourable vertical component of the crosswind.

#### *Longitudinal wake safety interval simulation*

In this study, the pilot reaction time is established as two seconds [20]. The analysis underlines that both vertical and lateral components of the crosswind are critical when evaluating longitudinal wake turbulence safety. The study focuses on the most disadvantageous vertical component of the crosswind, examining scenarios where the lateral component of the crosswind is set to 0 m/s and the vertical component to 0 m/s,

along with a scenario featuring a lateral component of 8 m/s. Figures 5 and 6 illustrate the resulting variations in the effective component of induced velocity at the wing centre of the trailing aircraft and the induced roll moment, respectively, in relation to changes in longitudinal separation. As can be seen from the figures, the effective component of induced velocity and induced roll moment remain minimal regardless of the longitudinal separation between the leading and trailing aircraft, thus not affecting the trailing aircraft’s operation. In calm lateral wind conditions, the wake vortex core does not drift laterally, ensuring a significant lateral distance from the trailing aircraft irrespective of its longitudinal movement. Similarly, in calm vertical wind conditions, the wake vortex core does not vertically approach the trailing aircraft, maintaining a substantial vertical separation regardless of the trailing aircraft’s longitudinal position.

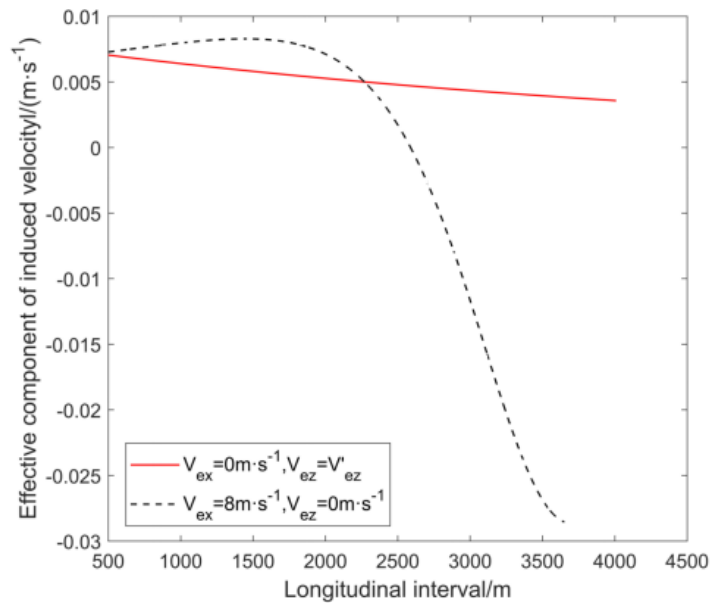


Figure 5 – Changes of effective component of induced velocity in unidirectional calm wind with longitudinal interval

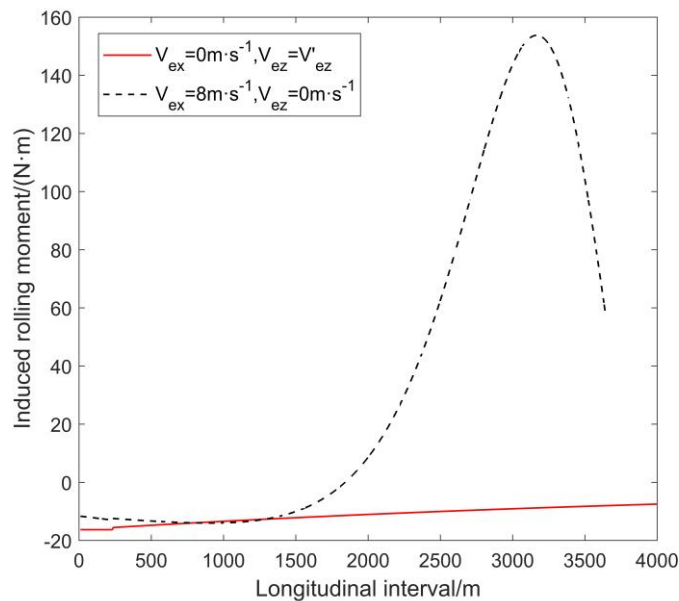


Figure 6 – Changes of induced roll moment in unidirectional calm wind with longitudinal interval

To analyse the longitudinal wake safety interval, the study considers the most disadvantageous vertical component of the crosswind, denoted as  $V'_{ez}$ , and examines scenarios with lateral components of the

crosswind set to 7 m/s, 8 m/s and 9 m/s. The variations in the effective component of induced velocity and the induced roll moment on the rear wing are depicted in *Figures 7 and 8*. Furthermore, when the centre of the rear wing aligns with the centre of the leading aircraft’s front right vortex core, the longitudinal interval extends from 0 m to a specified value.

The analysis reveals that the effective component of induced velocity and the induced roll moment at the centre point of the trailing aircraft’s wing change with the longitudinal interval. As the lateral component of the crosswind increases, the effective components of induced velocity and induced roll moment decrease, while the longitudinal separation corresponding to their maximum values increases. This occurs because a smaller lateral component of the crosswind allows more time for the leading aircraft’s wake to reach the trailing aircraft’s wing. Additionally, as the wake travels a greater distance longitudinally, its intensity gradually diminishes, resulting in reduced induced velocity and roll moment.

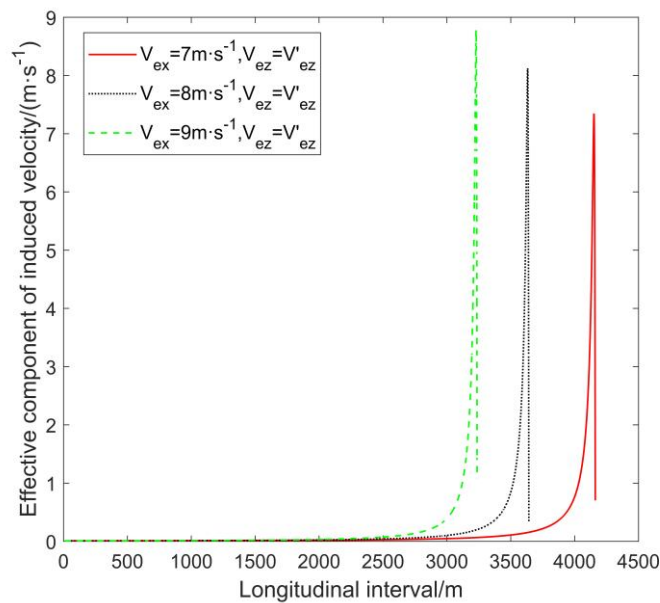


Figure 7 – Changes of the effective component of induced velocity with longitudinal interval

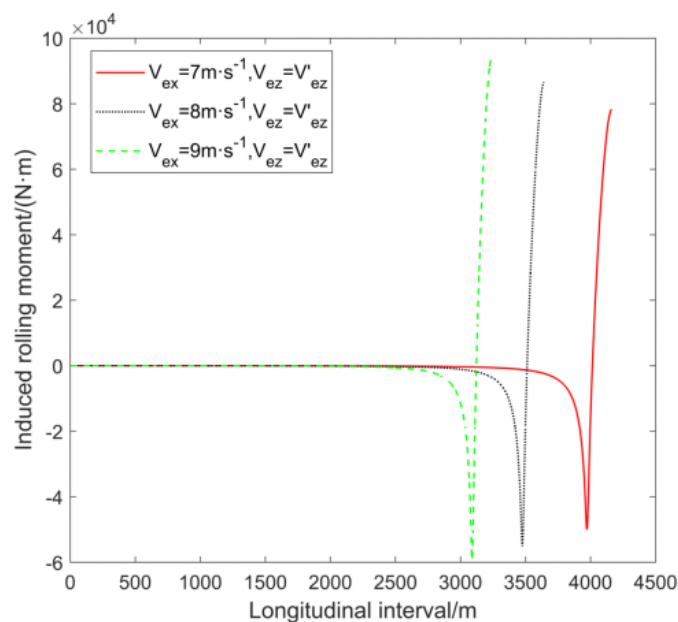


Figure 8 – Changes of induced roll moment on the trailing aircraft with longitudinal interval

Figure 9 illustrates the fluctuation of the maximum roll angle of the trailing aircraft within the longitudinal interval. In determining the longitudinal wake safety interval, the minimum longitudinal interval value is

identified at the point where the maximum roll angle equals  $10^\circ$  [23], as indicated by the red circle in *Figure 9*. This selection is crucial because if the longitudinal separation between the leading and trailing aircraft exceeds this value, the roll angle of the trailing aircraft will have surpassed the critical roll angle. Consequently, it becomes unfeasible for the aircraft to attain the subsequent longitudinal separation with a maximum roll angle of  $10^\circ$ .

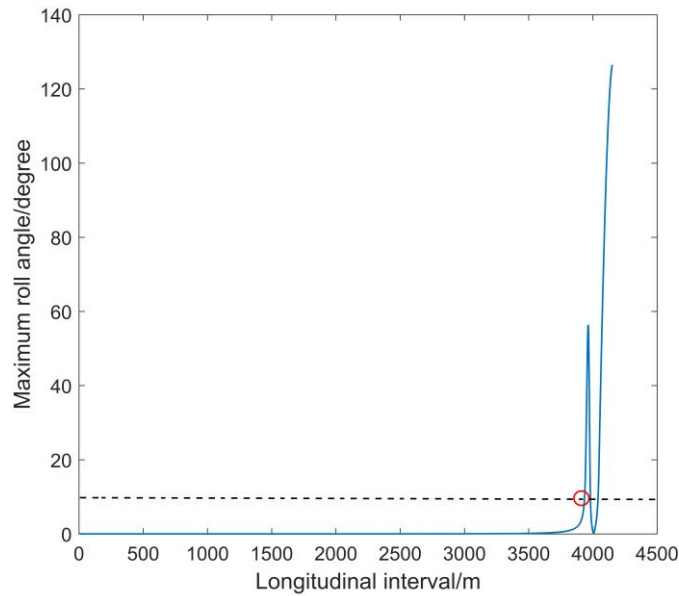


Figure 9 – Variation of maximum roll angle with longitudinal interval

*Figure 10* presents the calculated longitudinal wake safety interval during the approach process. It can be seen that the longitudinal wake turbulence safety separation progressively decreases, reaching its minimum value at the final moment. This decline results from the diminishing lateral separation between the leading and trailing aircraft as the paired approach nears completion, with the minimum lateral separation occurring at the end. As this lateral separation lessens, the distance between the vortex core and the trailing aircraft narrows. Consequently, the vortex core traverses a shorter longitudinal distance behind the trailing aircraft, thereby reducing the longitudinal wake turbulence safety separation. Additionally, an increase in the lateral component of the crosswind leads to a decrease in the wake turbulence safety separation. This is attributed to the fact that a stronger lateral component of the crosswind necessitates a smaller longitudinal separation for the vortex core to move the same lateral distance towards the trailing aircraft.

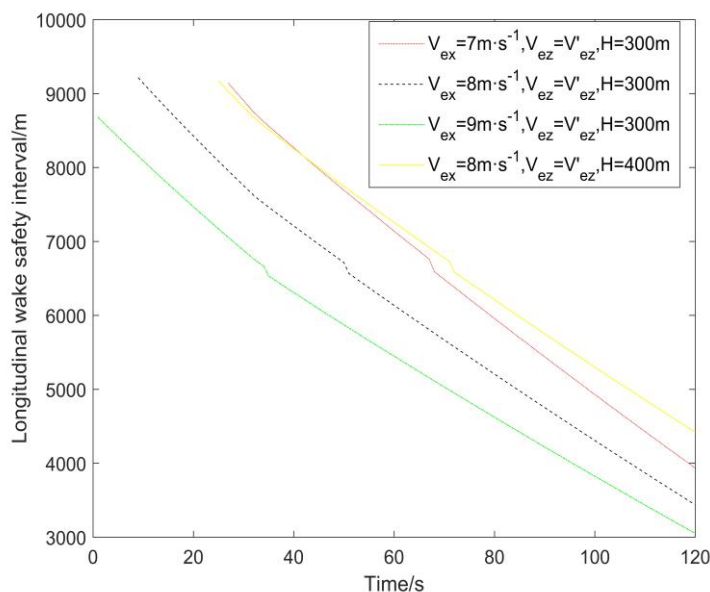


Figure 10 – Changes of longitudinal wake safety interval under different crosswinds

Furthermore, when  $V_{ex} = 7$  m/s and  $V_{ex} = 8$  m/s, there is initially no longitudinal wake safety interval during the early stages of the paired approach. This absence is attributed to the substantial lateral interval between the leading and trailing aircraft at the outset, requiring the wake vortex core to cover a longer longitudinal distance to approach the trailing aircraft. After travelling this extended distance, the intensity of the wake vortex core significantly diminishes, rendering the induced roll moment insufficient to elevate the roll angle of the trailing aircraft to the critical threshold.

The influence of varying runway intervals on the longitudinal wake safety interval is crucial to consider, as the lateral separation between the leading and trailing aircraft profoundly affects the longitudinal wake safety interval in a paired approach. For instance, as shown in *Figure 10*, a runway interval of 400 m results in a larger longitudinal safety interval compared to a 300 m interval. This difference arises because a larger runway interval effectively increases the lateral separation between the leading and trailing aircraft at each point during the paired approach. Consequently, the vortex core is compelled to traverse a greater lateral distance and subsequently a longer longitudinal path.

#### 4.2 CSPRs paired approach longitudinal collision risk analysis

The initial longitudinal interval is set at 2,000 m, with runway intervals at 300 m and 400 m and crosswind speeds at 7 m/s, 8 m/s and 9 m/s. Utilising the longitudinal collision risk model established earlier, in conjunction with the previously analysed longitudinal wake safety interval, the longitudinal collision risk during the paired approach is calculated, as depicted in *Figure 11*.

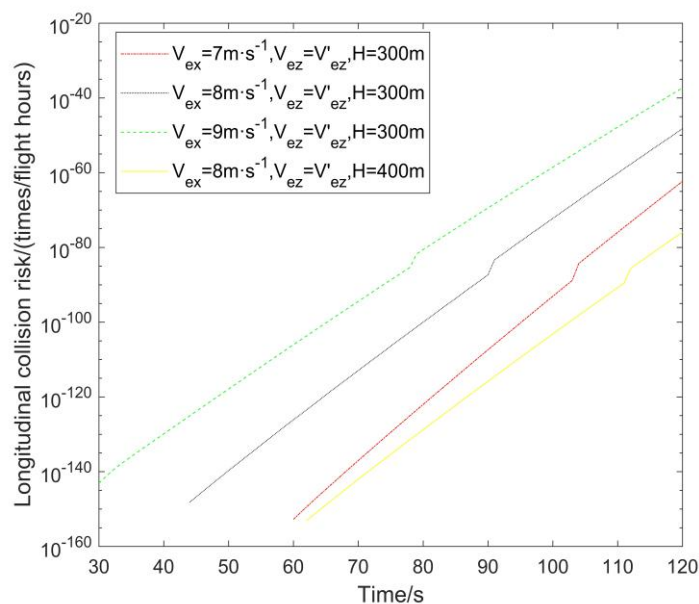


Figure 11 – Variation of longitudinal collision risk with time under different crosswinds and runway intervals

The International Civil Aviation Organization (ICAO) specifies a safety target level of  $5 \times 10^{-9}$  times/flight hour for longitudinal directions [24]. Based on the longitudinal collision risk values in *Figure 11*, the paired approach process meets ICAO's safety target level under these parameters, indicating the feasibility of the current longitudinal wake safety interval.

As shown in *Figure 11*, the longitudinal collision risk escalates over time, peaking at the final moment. This increase corresponds with the time-dependent decrease in the longitudinal wake safety interval, which reaches its minimum at the end. Consequently, the likelihood of the trailing aircraft's position falling beyond the wake safety interval increases. Despite the continuous decrease in the longitudinal interval between the two aircraft during the paired approach, its instantaneous variation is significantly smaller than that of the longitudinal wake safety interval. *Figure 11* also reveals that the longitudinal collision risk value escalates with an increase in the lateral component of the crosswind and diminishes as the runway interval increases. This trend occurs because larger crosswind components and smaller runway intervals result in a reduced longitudinal wake safety interval, thereby heightening the longitudinal collision risk.

Analysing the data in *Figure 12*, where the runway interval is set at 300 m, the lateral wind speed of the crosswind is 7 m/s and the initial longitudinal intervals are 2000 m, 2500 m and 3000 m, it is possible to



observe the variation in longitudinal collision risk over time. An increase in the initial longitudinal interval corresponds to a continuous rise in longitudinal collision risk. This correlation arises because a larger initial longitudinal interval implies a greater theoretical separation between the two aircraft. Consequently, there is an increased likelihood of the trailing aircraft's position extending beyond the wake safety interval, thereby elevating the risk of longitudinal collision.

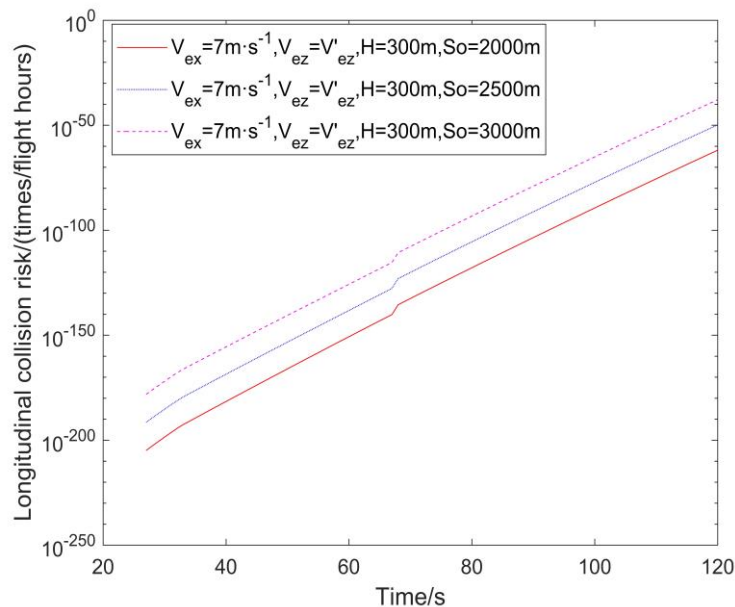


Figure 12 – Variation of longitudinal collision risk with time under different initial longitudinal intervals

## 5. CONCLUSIONS

This paper presents a new perspective in CSPRs paired approach collision risk research by acknowledging that the trailing aircraft does not necessarily have to strictly avoid the wake of the leading aircraft. It posits that safe paired approaches can still be executed even when the trailing aircraft continuously operates within the wake of the leading aircraft. The related research is carried out as follows:

Firstly, based on QAR data, the motion process of conventionally approaching aircraft is analysed, and the velocity change of the paired aircraft is divided into two stages of uniform deceleration. Based on this analysis, a theoretical interval model of the paired aircraft is established. Secondly, the acceleration error is statistically analysed, revealing that the mixed Laplace distribution is most consistent with the distribution of acceleration deviation values. Thus, it is selected as the acceleration error distribution. It is then considered that the trailing aircraft can withstand a certain intensity of the leading aircraft's wake stream, leading to the establishment of a wake stream safety interval calculation model. Model calculations show that longitudinal wake spacing exists only when both the lateral and vertical components of the crosswind are present simultaneously. Finally, based on probabilistic theory, assuming that the acceleration errors between the two paired aircraft are independent and without considering differences in operating conditions, a longitudinal collision risk calculation model is established. It is concluded that the longitudinal collision risk increases during the paired approach, reaching its maximum at the final moment. Additionally, the longitudinal collision risk decreases with increasing runway spacing and increases with the lateral component of the crosswind.

## REFERENCES

- [1] Waller MC, Scanlon CH. *Proceedings of the NASA workshop on flight deck centered parallel runway approaches in instrument meteorological conditions*. NASA. Report number: NAS 1.55:10191, 1996.
- [2] Hammer J. Study of the geometry of a dependent approach procedure to closely spaced parallel runways. *Proceedings of 18th Digital Avionics Systems Conference, 24-29 Oct. 1999, St. Louis, MO, USA*. 1999. p. 4.C.3-4.C.3. DOI: 10.1109/DASC.1999.863731.

- [3] Hammer J. Case study of paired approach procedure to closely spaced parallel runways. *Air Traffic Control Quarterly*. 2000;8(3):223–252. DOI: 10.2514/atcq.8.3.223.
- [4] Landry S, Prichett AR. The safe zone for paired closely spaced parallel approaches: implications for procedures and automation. *Proceedings of the 19th Digital Avionics Systems Conference (DASC), 7-13 Oct. 2000, Philadelphia, PA, USA*. 2000. p. 3E3/1–3E3/8. DOI: 10.2514/atcq.8.3.223.
- [5] Burnham DC, Hallock JN, Greene GC. Wake turbulence limits on paired approaches to parallel runways. *Journal of Aircraft*. 2002;39(4):630-637. DOI: 10.2514/6.2000-4128.
- [6] McKissick B. Wake encounter analysis for a closely spaced parallel runway paired approach simulation. *Proceedings of the 9th AIAA Aviation Technology, Integration, and Operations Conference (ATIO) and Aircraft Noise and Emissions Reduction Symposium (ANERS), 21–23 Sep. 2009, Hilton Head, SC, USA*. 2009. p. 6943. DOI: 10.2514/6.2009-6943.
- [7] Liu Y. Discussion on the feasibility of pairing approach with close parallel runways. *Air Traffic Management*. 2009;(10):4-5. DOI: JournalArticle/5af483f0c095d718d81a9f50.
- [8] Guerreiro N, et al. Characterizing a wake-free safe zone for the Simplified Aircraft-based Paired Approach concept. *Proceedings of the AIAA Atmospheric and Space Environments Conference, 2–5 Aug. 2010, Toronto, ON, CAN*. 2010. p. 7681. DOI: 10.2514/6.2010-7681.
- [9] Guerreiro N, Neitzke K. Simulated wake characteristics data for closely spaced parallel runway operations analysis. *Proceedings of the 12th AIAA Aviation Technology, Integration, and Operations (ATIO) Conference and 14th AIAA/ISSMO Multidisciplinary Analysis and Optimization Conference, 17–19 Sep. 2012, Indianapolis, IN, USA*. 2012. p. 5642. DOI: 10.2514/6.2012-5642.
- [10] Lu F, et al. Longitudinal collision risk safety assessment of paired approach to closed spaced parallel runways. *China Safety Science Journal*. 2013;(08):108–113. DOI: 10.16265/j.cnki.issn1003-3033.2013.08.011.
- [11] Lu F, et al. Assessment of lateral collision risk in closed spaced parallel runways paired approach. *China Safety Science Journal*. 2016;(11):87–92. DOI: 10.16265/j.cnki.issn1003-3033.2016.11.016.
- [12] Lu F, et al. Lateral collision risk of CSPRs paired approach under wake impact. *China Safety Science Journal*. 2016;(02):99–105. DOI: 10.16265/j.cnki.issn1003-3033.2020.02.016.
- [13] Lu F, et al. Lateral collision dynamics of CSPRs paired approach under influence of wake vortex field. *China Safety Science Journal*. 2020;30(4):21-27. DOI: 10.16265/j.cnki.issn1003-3033.2020.04.004.
- [14] Tian Y, et al. Method for determining the distance between close parallel runways. *Journal of Traffic Transportation Engineering*. 2013;(01):70–76. DOI: 10.19818/j.cnki.1671-1637.2013.01.011.
- [15] Domino DA, et al. Paired approaches to closely spaced runways: Results of pilot and ATC simulation. *Proceedings of the 2014 IEEE/AIAA 33rd Digital Avionics Systems Conference (DASC), 5–9 Oct. 2014, Colorado Springs, CO, USA*. 2014. p. 1B2-1–1B2-15. DOI: 10.1109/DASC.2014.6979548.
- [16] Leiden K, et al. Paired approach flight demonstration: Planning and development activities. *Proceedings of the 2018 Integrated Communications, Navigation, Surveillance Conference (ICNS), 10–12 Apr. 2018, Herndon, VA, USA*. 2018. p. 3G4-1–3G4-12. DOI: 10.1109/ICNSURV.2018.8384963.
- [17] Leiden K, et al. Paired approach flight demonstration results. *Proceedings of the 2019 Integrated Communications, Navigation and Surveillance Conference (ICNS), 9–11 Apr. 2019, Herndon, VA, USA*. 2019. p. 1–16. DOI: 10.1109/ICNSURV.2019.8735116.
- [18] Wei Z, Wu J, Liu X, Li N. Safety assessment and analysis on standard of wake separation for air traffic. *Journal of Safety Science Technology*. 2018;(12):180–185. DOI: CNKI:SUN:LDBK.0.2018-12-030.
- [19] Han J, et al. Large eddy simulation of aircraft wake vortices within homogeneous turbulence- Crow instability. *AIAA Journal*. 2000;38(2):292–300. DOI: 10.2514/2.956.
- [20] Zhang X. *Modeling and simulation of dynamic visual characteristics and control characteristics of pilots in cockpit*. PhD thesis. Northwestern Polytechnical University; 2017.
- [21] Kuang J, Wang B. *Flight dynamics*. Beijing, China: Tsinghua University Press; 2012.
- [22] Wei Z. *The research on modeling and simulation of flow field and safety spacing for wake vortex*. PhD thesis. Civil Aviation University of China; 2009.
- [23] Luckner R, Höhne G, Fuhrmann M. Hazard criteria for wake vortex encounters during approach. *Aerospace Science and Technology*, 2004; 8(8):673-687. DOI: 10.1016/j.ast.2004.06.008.
- [24] International Civil Aviation Organization. *Doc8168 OPS/611: Construction of Visual and Instrument Flight Procedures*. Montreal, CAN: ICAO; 2007.

卢飞 张健 赵二丽 滕景杰

### 近距平行跑道配对进近纵向碰撞风险研究

#### 摘要:

本文考虑配对后机可以承受一定程度的前机尾流,对近距平行跑道配对进近纵向碰撞风险进行研究,目的是扩大配对进近过程中的安全范围,便于配对进近的灵活实施。基于 QAR 数据建立配对飞机的理论间隔模型和加速度误差的概率分布,进而得出配对两机的实际间隔分布。通过大涡模拟的方法对尾流强度的衰减进行仿真,建立尾流的衰减模型;基于经典 Hallock-burnham 涡模型建立了配对前机尾流的诱导速度计算模型和涡核运动模型。考虑到后机可以承受一定强度的尾流,以最大滚转角等于临界滚转角为限制建立了尾流安全间隔计算模型。最后基于概率论理论,结合尾流安全间隔计算模型和配对飞机对的实际间隔分布建立了纵向碰撞风险计算模型。本研究也对不同因素对纵向碰撞风险的影响进行了分析,结果表明:研究纵向尾流安全性时,必须存在侧风环境条件才有意义;侧风侧向分量越大,尾流安全间隔越小。纵向碰撞风险在配对进近过程中不断增大并在最后时刻达到最大值;纵向碰撞风险随侧风侧向分量和初始纵向间隔的增大而增大,随跑道间隔的增大而减小。

#### 关键词:

配对进近;碰撞风险;尾涡流场;安全间隔;加速度误差;滚转力矩